Available online at www.dergipark.org.tr/en

INTERNATIONAL ADVANCED RESEARCHES and ENGINEERING JOURNAL

Journal homepage: www.dergipark.org.tr/en/pub/iarej

e-ISSN: 2618-575X

International Open Access

Volume 09
Issue 01

April, 2025

Research Article

Study of synthesis, structure and temperature-dependent phase evolution of Barium Zirconium Titanate

***Pelin Sözen Aktaş*[a,*]**

[a]*Manisa Celal Bayar University, Faculty of Engineering and Natural Sciences, Department of Chemistry, Şehit Prof. Dr. İlhan Varank Campus, Muradiye-Manisa, 45140, Türkiye*

ARTICLE INFO

Article history:
Received 14 November 2024
Accepted 11 April 2025
Published 23 April 2025

Keywords:
Barium zirconium titanate
Organic titanate
Pechini
X-ray diffraction

ABSTRACT

In this study, Barium Zirconium Titanate ($BaZr_xTi_{1-x}O_3$) (where x=0.1 and 0.2) structures were synthesized using starting materials of barium acetate, titanium (triethanolaminato) isopropoxide (80% w/w in isopropanol), and Zr(IV)propoxide (70% 1-propanol solution) through the Pechini method. The significance of this synthesis lies in its novel application of commercially available, air-stable organic titanate precursors. The BZT structures were characterized using X-ray diffraction (XRD), Fourier Transform Infrared spectroscopy (FT-IR), Thermal Gravimetric Analysis (TGA), and Scanning Electron Microscopy with Energy Dispersive X-ray (SEM-EDX) analyses. XRD patterns of the resultant samples, taken after calcination processes at temperatures ranging from 800°C to 1200 °C, support the hypothesis that zirconium is integrated into the structure. SEM results demonstrated that as the amount of Zr increased, the grain size of BZT decreased, with BZT2 particles exhibiting a spherical morphology. The grain sizes of the BZT2 sample ranged approximately from 180 to 50 nm. Furthermore, EDX analyses confirmed the substitution of Zr within the BZT structure.

1. Introduction

The remarkable optical and electrical properties of lead-based perovskites have attained great success, but the instability and toxicity of Pb-based perovskites keep them out of commercial applications. This concern for environmental safety has significantly shifted towards lead-free materials.

Barium titanate is recognized as the most prominent and environmentally friendly ferroelectric ceramic within the perovskite family. Among the most appealing systems derived from this perovskite family are barium zirconium titanate, barium strontium titanate, and dopped metals of BT systems.

Barium zirconate titanate systems (BZT) are among the most significant of these, and they are noted for their extensive applications in the production of energy-consuming devices in areas such as electronics and communications. By focusing on lead-free materials like BZT, we can contribute to the global effort for environmental safety. [1-4]. Barium zirconium titanates are recognized as excellent materials for dielectrics used in industrial micro-electro-mechanical systems, capacitors, and dynamic random-access memory systems. [5, 6]. BZT ceramic materials are commonly expected to be promising for piezoelectric actuators and sensors [7]. BZT systems originated from barium titanate (BT) and barium zirconate (BZ) lattices, where zirconium replacements to titanium lattices have been stated to enhance dielectric and piezoelectric properties [8-11]. The replacement of Ti^{4+} by stable and large cations like Zr^{4+} leads to the diffuse phase transition. It has been stated that Zr^{4+} substitution in the Ti^{4+} region is a helpful way to lower the Curie temperature. Compared to Ti^{4+}, the Zr^{4+} ion is larger and is more stable. By replacing titanium(IV) with zirconium(IV), the perovskite lattice becomes more expansive, and the leakage current is reduced because of electron jumping between Ti^{4+} and Ti^{3+} [12, 13]. The substitution of Zr^{4+} ions significantly improves the basic properties of barium titanate [14]. Barium Zirconium Titanate (BZT) ceramics have outstanding dielectric properties, including improved leakage current, low dielectric loss, dielectric constant, and lowered transition temperature. These features of BZT open various potential applications, from actuators and

* Corresponding author. Tel.:+90-236-201-3182; Fax: +90-236-201-2020.
E-mail addresses: pelin.sozen@cbu.edu.tr *(P. Sözen Aktaş)*
ORCID: 0000-0003-2140-2650 *(P. Sözen Aktaş)*
DOI: 10.35860/iarej.1585507

capacitors to sensors, tunable microwave devices, and antennas. The promising properties of BZT suggest a bright future for its use in various electronic and communication devices. [3, 9, 15, 16]. However, while the product is being developed, obtaining a homogeneous, fine particle-size material should be at the forefront. Under common preparation conditions, these materials usually have heating, calcining, and sintering at high temperatures [11]. To date, many techniques have been developed for synthesizing barium zirconium titanates. These synthesis techniques are divided into three groups: solid state, liquid state, and gas state. While solid-state methods are used for bulk material synthesis, liquid-state techniques have gained importance for nanomaterial production [17].

Barium zirconium titanate is traditionally synthesized through a solid-state reaction involving barium carbonate, titanium(IV) oxide, and zirconium(IV) oxide at elevated temperatures [18, 19]. This conventional approach is inadequate because of issues related to the milling process and contamination during the sintering and calcination stages. Liquid state techniques frequently used in synthesizing barium zirconium titanate are solid state, auto-combustion, sol-gel, Pechini, and co-precipitation [20-23]. Among these, the Pechini method is preferred due to its simplicity, homogeneous distribution, complex oxide, and nanometric product formation [10, 24, 25]. In the previous investigation, the synthesis of nano-scale round-shaped barium titanate via the Pechini technique using an organic titanate complex of triethanolaminato was reported by Aktaş [26].

This study concentrates on synthesizing homogeneous BZT structures at reduced temperatures, employing stable precursor materials, including barium acetate, zirconium propoxide, and an organic titanium complex. Furthermore, the use of Ti(IV) (triethanolaminato) isopropoxide as a starting material for synthesizing TiO_2, $BaTiO_3$, and metal titanates has been documented in a limited number of studies. [27-30]. Upadhyay and co-workers prepared spherical and cubic nanoparticles of $BaTiO_3$ via Ti-triethanolamine isopropoxide and barium hydroxide in MeOH solution [27]. As an alternative to metallic alkoxides, using metal complexes in liquid-phase reactions allows for obtaining nano-scale structures. In the present work, ($BaZr_xTi_{1-x}O_3$) (x=0.1 (BZT1), x=0.2 BZT2) structures were synthesized via the Pechini technique. However, no literature has been published on synthesizing BZT with a titanium triethanolaminato complex.

The primary advantage of this synthesis lies in its unique utilization of a commercially available, air-stable organic titanate precursor, marking a significant advancement in the field. The characterization and phase formation of the prepared BZT1 and BZT2 samples are elucidated through TGA, FTIR, XRD, and SEM analyses. The structural properties and morphology of the samples are also studied. The results obtained from XRD and SEM indicated a correlated increase in mole fraction, influenced by higher calcination temperatures and reduced grain size.

2. Experimental

2.1 Materials and Method

Barium acetate; ($Ba(CH_3COO)_2$, 99 %, Sigma-Aldrich), Zirconium(IV)propoxide solution ($Zr(OCH_2CH_2CH_3)_4$, 70 wt.% in 1-propanol, Aldrich), titanium (triethanolaminato) isopropoxide solution (80 wt.% in isopropanol, Sigma Aldrich), citric acid ($C_6H_8O_7$, ≥ 99.5%, Sigma-Aldrich), ethylene glycol ($C_2H_6O_2$, 99.8%, Sigma-Aldrich) and were used as starting materials. The BZT powders were characterized utilizing X-ray diffraction (XRD) with a PANalytical Empyrean diffractometer operating within a 2θ range of 10 ° to 80 °, at a scan speed of 0.05 ° s^{-1}, employing λ = 1.5406 Å Cu Kα radiation. The phase identification was conducted using the Match! Program (Version 3, Crystal Impact). [31]. The FT-IR spectra of the powders were obtained using an FT-IR spectrometer (Spectrum BX Perkin Elmer), scanning from 4000 cm-1 to 400 cm-1 with the KBr disc method. The Spectragryph Software for Optical Spectroscopy Version 1.2.16.1 was examined for spectrum graphs. [32]. TGA analysis instrument SII 7300 Perkin Elmer thermal analyzer was used to understand the thermal stability of samples. A Zeiss Gemini 500 microscope was employed to analyze the morphology of the BZT structure. The analysis of the elemental composition of the BZT samples was conducted utilizing EDX.

2.2 Synthesis of Barium Zirconium Titanate samples

$Ba(Zr_{0.1}Ti_{0.9})O_3$ (BZT1) and $Ba(Zr_{0.2}Ti_{0.8})O_3$ (BZT2) samples were synthesized using the Pechini technique. The experimental pathway is presented in Figure 1.

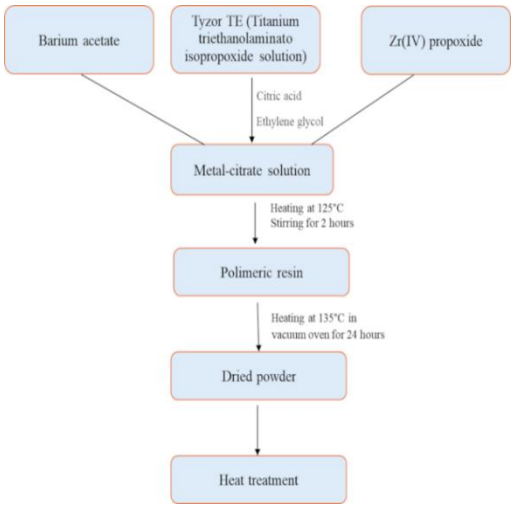

Figure 1. Synthesis pathway of BZT powders using the Pechini method.

The synthesis procedure is given for $Ba(Zr_{0.1}Ti_{0.9})O_3$ (BZT1). In the first stage, the metallic citrate solutions were prepared using barium acetate (4.0g, 15.66mmol), titanium(IV) (triethanolaminato) isopropoxide (4.45 g, 14.09 mmol), Zr(IV)propoxide (in 70 % 1-propanol, 0.7 mL, 1.56 mmol), citric acid (13.53 g, 70 mmol) and ethylene glycol (17.46 mL, 313.2 mmol). The molar ratio is Ba/ $(Zr_{0.1}Ti_{0.9})$/ citric acid/ ethylene glycol = 1/ 1/ 4.5/ 20. The solution was maintained at 125 °C for 2 hours to produce a clear, pale-yellow gel. Subsequently, this gel was heated at 135 °C in a vacuum oven for 24 hours. The resulting powder underwent a two-step heating process: initially, it was treated at 400 °C for 4 hours to eliminate organic residues, followed by treatment at temperatures ranging from 800 to 1200 °C for an additional 4 hours at a heating rate of 5 °C per minute, before being allowed to cool to room temperature. The synthesis of $Ba(Zr_{0.2}Ti_{0.8})O_3$ (BZT2) was prepared in the same pathway using the appropriate stoichiometric ratio.

3. Results and Discussion

3.1 TGA and FTIR Analysis

The thermal analysis of the BZT1 precursor, which was acquired at a temperature of 135 °C and subsequently dried, was conducted using TGA with a heating rate of 10 °C per minute, extending to a maximum temperature of 1400 °C. The TGA curve for BZT1 (refer to Figure 2) indicates an initial mass loss of 9% within the temperature range of 25 °C to 200 °C, which is attributable to the moisture and volatiles adsorbed by the sample [33]. The subsequent mass loss observed between 200 °C and 550 °C is associated with the dehydration of organic molecules [23]. Ultimately, in the temperature range of 1050 °C to 1400 °C, the weight of the powder remains relatively stable. Following calcination at 1050 °C, a residue comprising 16.5% was obtained. A comparable scenario is evident in the TGA curve for BZT2 (as illustrated in Figure 2), where the weight of the powder also remains nearly constant between 1060 °C and 1400 °C. Notably, after calcination at 1060 °C, the residue for BZT2 was approximately 14%.

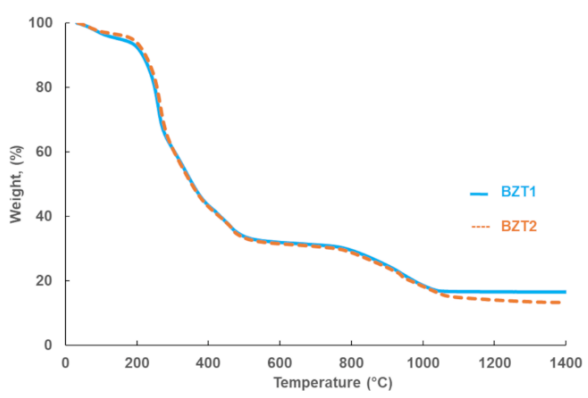

Figure 2. TGA plot of as-prepared BZT1 and BZT2 precursors.

The FTIR analyses were employed to determine the vibration peaks of zirconium and titanium oxygen bonds. Figure 3 illustrates the FT-IR spectrum of the BZT powders calcined at 1200 °C. In the FTIR spectrum of BZT1 and BZT2, the vibration bands between 500-600 cm^{-1} can be assigned to Ti-O and Zr-O stretching vibrations [34]. The absorption bands at 574 cm^{-1} and 531 cm^{-1} are assigned to Ti-O and Zr-O vibration bands of MO_6 (M=Ti or Zr) in BZT2. In BZT1, with a smaller amount of Zr doped, a single broad stretching vibration peak was observed at 537 cm^{-1}.

3.2 XRD Analysis and Temperature-dependent Phase Evolution

In this study, the structure of Zr-substituted BT has been investigated to understand the structural shift by adding Zr in BT. The resulting powder sample was heated at 5 °C/min at calcination temperatures of 800°C to 1200 °C. The XRD pattern of BZT1 powder obtained by the Pechini method at 800 °C is shown in Figure 4. $BaCO_3$ was typically observed due to the open-air system. The peaks were observed for the BT, BZ, and Zr-doped BZT samples at 800 °C.

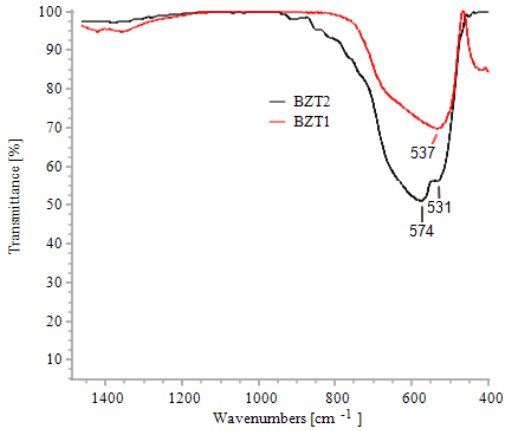

Figure 3. FTIR spectrum of BZT1 and BZT2 samples prepared at 1200 °C.

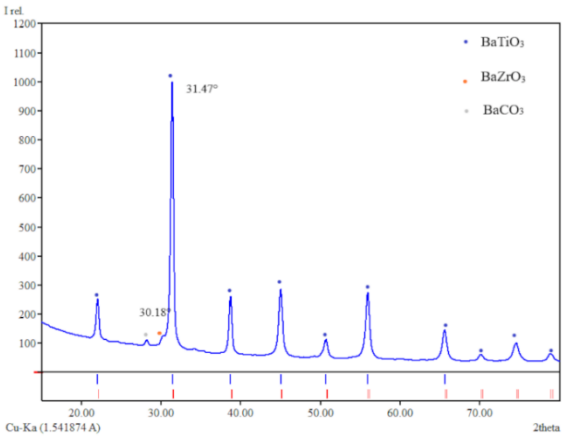

Figure 4. XRD pattern of $BaZr_{0.1}Ti_{0.9}O_3$ sample calcined at 800 °C. (JCPDS no.79-2263 $BaTiO_3$ (BT), JCPDS no. 74-1299 $BaZrO_3$ (BZ))

Due to the inability of Zirconium to diffuse, it is imperative to elevate the calcination temperature to attain a greater Zr content. Consequently, a single phase was successfully achieved at elevated temperatures of 900°C, 1000 °C, and 1200 °C, as illustrated in Figures 5 and Figure 6. BZT1 and BZT2 were obtained at 1000 °C and 1200 °C respectively. The diffraction peaks of BZT1 and BZT2 exhibit a shift towards lower angles, while the full width at half maximum (FWHM) of the XRD peaks increases with the augmentation of zirconium content. At BZT2, the reflection peaks shifted towards lower 2θ, suggesting that the Zr^{4+} ion is substituted to the Ti-site. The shift of 110 diffraction peak values for BZT1 and BZT2 are given in Table 1.

Table 1. The shift of 110 peaks is a result of the temperature variation.

	800 °C	900 °C	1000 °C	1200 °C
BZ	30.29	30.19	-	-
BT	31.41	31.48	-	-
BZT1	-	-	30.77	31.29
BZ	30.26	30.24	-	-
BT	31.41	31.38	-	-
BZT2	-		31.19	31.19

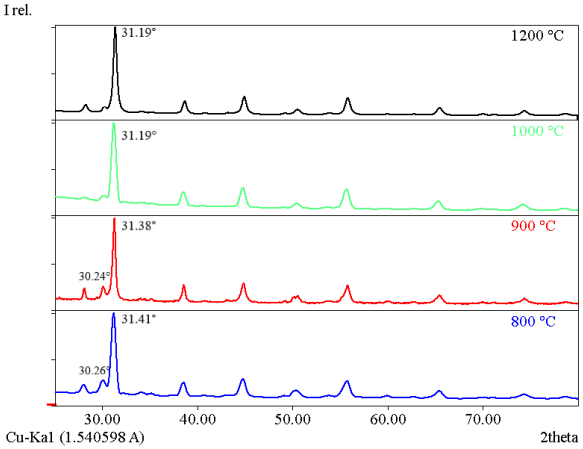

Figure 5. XRD patterns of BZT1 powder after calcination at 800°, 900°C, 1000° C and 1200° C.

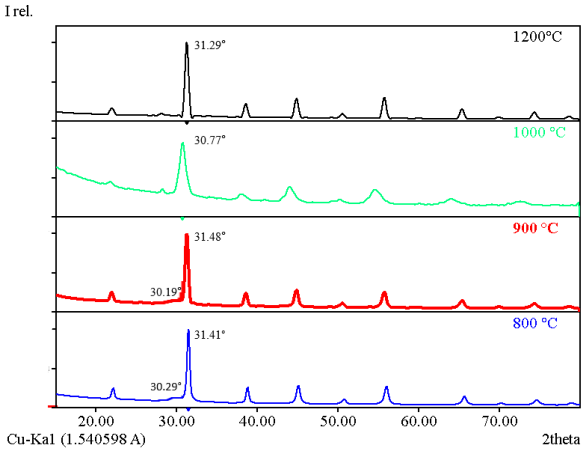

Figure 6. XRD patterns of BZT2 powder after calcination at 800°, 900°C, 1000° C and 1200° C.

3.3 EDX and SEM Analysis

EDX analysis was conducted on Barium Zirconate Titanate (BZT) samples to elucidate their chemical composition. The resulting spectrum indicates the presence of the element's barium, zirconium, titanium, and oxygen. It was observed that the percentage elemental values closely corresponded to both the calculated and experimental values. The EDX analysis, as illustrated in Figure 7, demonstrates that the obtained BZT powders were nearly identical to the intended stoichiometry during preparation, and no traces of any extraneous elements were detected.

SEM images of BZT1 and BZT2 are presented in Figure 8. This figure illustrates the microstructures of the BZT1 and BZT2 samples that have been calcined at 1200 °C. It is evident that zirconium substitutions significantly influence the morphology and grain size of the samples. Observations indicate that the average grain sizes decrease from 200-120 nm to 180-50 nm as the Zr fraction is increased. Similar findings were reported by Reda and colleagues [35]. The reduction in grain size can be ascribed to a decreased grain growth rate during calcination, which results from the slow atomic diffusion of Zr ions. The grain morphology of the BZT1 samples transforms from blocky and various pentagonal and partially irregular shapes to more rounded configurations, as evidenced in the structure of BZT2.

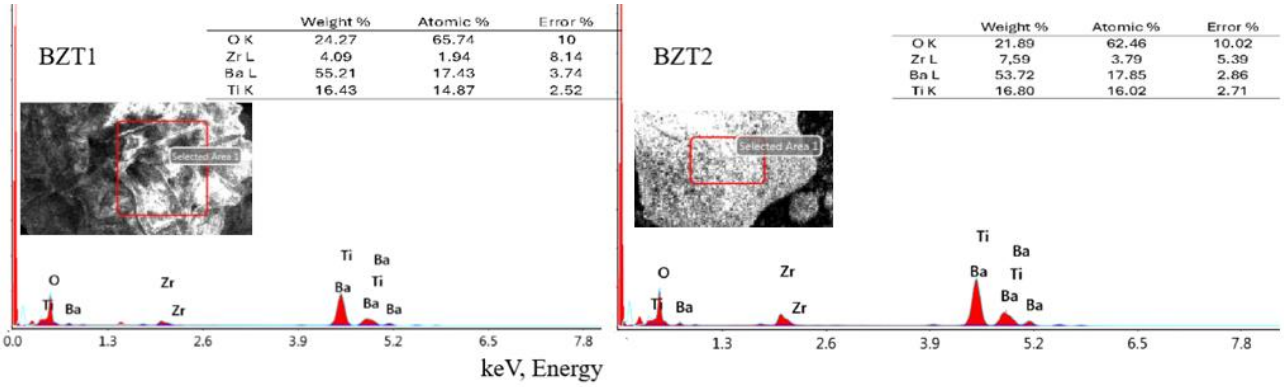

Figure 7. EDX spectrum of BZT1 and BZT2 samples calcined at 1200 °C

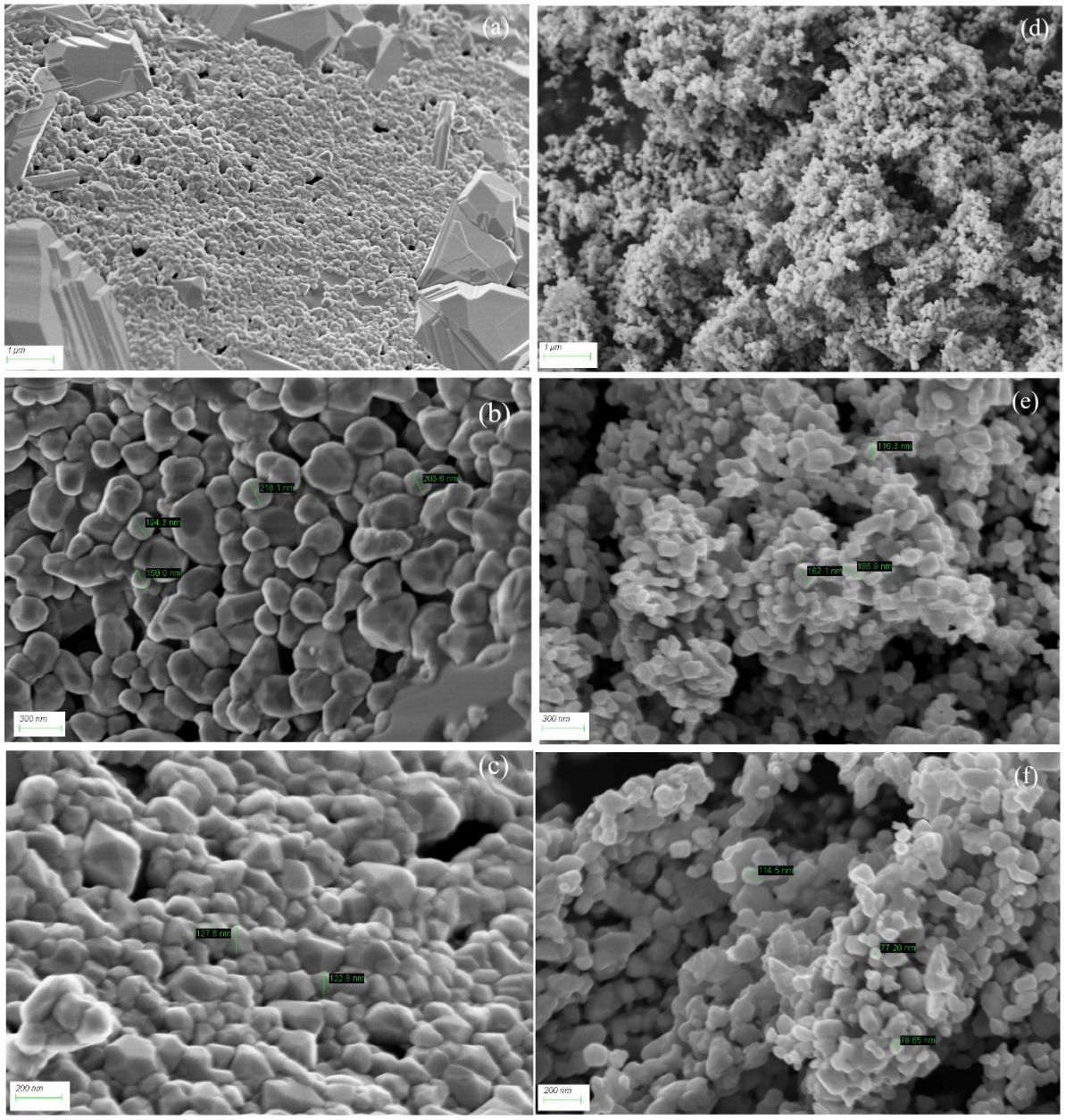

Figure 8. The SEM micrograph of BZT1 (a, b, c) and BZT2 (d, e, f) samples calcined at 1200 °C.

4. Conclusion

In the present study, barium zirconium titanates ($BaZr_xTi_{1-x}$, where x = 0.1, 0.2) with varying zirconium contents were synthesized utilizing the Pechini method. The titanium source employed was titanium (triethanolaminato) isopropoxide, noted for its stability in atmospheric conditions, economic viability, and commercial availability. This precursor offers several advantages over other titanium sources, including titanium chloride or propoxide, typically employed in liquid-phase synthesis methods.

The phase evolution is monitored through XRD measurements, and the results confirm establishing a single BZT form at temperatures exceeding 1000°C. The calcination of samples at 1200°C allowed the Zr^{+4} ions to diffuse into the lattice structure of barium titanate. The results from XRD and SEM indicated a rise in mole fraction, which is influenced by the elevated calcination temperature and the reduction in grain size. Also, XRD results demonstrated Zr ions successfully incorporated into lattice structure as confirmed by shifts at 2θ. It is observed that the average grain size decreased from 200-120 nm for BZT1 to 180-50 nm for BZT2 with increasing the Zr fraction.

Declaration

The author confirmed no potential conflicts of interest related to this research, authorship, or publication. Additionally, the author indicated that this article is original and was prepared in accordance with international publication and research ethics; no ethical committee permission or special approval is necessary.

Author Contributions

P. Sözen Aktaş developed the manuscript's conceptualization, methodology, validation, and presentation.

Acknowledgment

The author acknowledged support from the Manisa Celal Bayar University Research Projects Commission. (Project number: 2019-056).

References

1. Qiu, J.H., T.X. Zhao, Z.H. Chen, X.Q. Wang, N.Y. Yuan, and J.N. Ding, *Phase diagram and physical properties of (110) oriented $Ba(Zr_{0.08}Ti_{0.92})O_3$ thin film.* Solid State Communications, 2019. **289**: p. 1–4.
2. Kaur, R., M. Singh, and A. Singh, *Influence of samarium and iron substitution on structural and electrical properties of barium zirconate titanate solid solutions.* Journal of Asian Ceramic Societies, 2019. **7**(3): p. 284–297.
3. Maiti, T., R. Guo, and A.S. Bhalla, *Enhanced electric field tunable dielectric properties of $BaZr_xTi_{1-x}O_3$ relaxor ferroelectrics*. Applied Physics Letters, 2007. **90**(18): p.182901.
4. Delibaş, N. C., S. B. Gharamaleki, M. Mansouri, and A. Niaie, *Reduction of operation temperature in SOFCs utilizing perovskites: Review*, International Advanced Researches and Engineering Journal, 2022. **6**(1): p. 56–67.
5. Ciomaga, C.E., M.T. Buscaglia, M. Viviani, V. Buscaglia, L. Mitoseriu, A. Stancu, P. Nanni, *Preparation and dielectric properties of $BaZr_{0.1}Ti_{0.9}O_3$ ceramics with different grain sizes.* Phase Transitions, 2006. **79**(6–7): p. 389–397.
6. Mangaiyarkkarasi, J., S. Sasikumar, O.V. Saravanan, and R. Saravanan, *Electronic structure and bonding interactions in $Ba_{1-x}Sr_xZr_{0.1}Ti_{0.9}O_3$ ceramics*. Frontiers of Materials Science, 2017. **11**(2): p. 182–189.
7. Dong, L., D.S. Stone, and R.S. Lakes, *Enhanced dielectric and piezoelectric properties of $xBaZrO_3$-(1-x)$BaTiO_3$ ceramics*. Journal of Applied Physics, 2012. **111**(8): p.084107.
8. Fahad, M., R. Thangavel, and P.M. Sarun, *Scaling behavior of the $BaZr_{0.1}Ti_{0.9}O_3$ (BZT) dielectric ceramic at the elevated temperatures (400 °C – 540 °C)*. Materials Science and Engineering B: Solid-State Materials for Advanced Technology, 2022. **283**: p.115837.
9. Bhargavi, G.N., T. Badapanda, M.S. Anwar, M. Tlija, H. Joardar, and S.N. Tripathy, *Understanding the impact of gadolinium substitution on the impedance and conduction mechanism of barium zirconium titanate ceramics.* Journal of Materials Science: Materials in Electronics, 2024. **35**(1991): p. 1-28.
10. Salem, M.M., M.A. Darwish, A.M. Altarawneh, Y.A. Alibwaini, R. Ghazy, O.M. Hemeda, D. Zhou, E.L. Trukhanova, A.V. Trukhanov, S.V. Trukhanov and M. Mostafa, *Investigation of the structure and dielectric properties of doped barium titanates*. RSC Advances, 2024. **14**(5): p. 3335–3345.
11. Kholodkova, A.A., A. V. Reznichenko, A.A. Vasin, and A. V. Smirnov, *Methods for the synthesis of barium titanate as a component of functional dielectric ceramics*. Tonkie Khimicheskie Tekhnologii, 2024. **19**: p. 72–87.
12. Jia, Q., B. Shen, X. Hao, J. Zhai, and X. Yao, *Enhanced dielectric property from highly (100)-oriented barium zirconate titanate compositional gradient films*. Thin Solid Films, 2010. **518**: p. e89–e92.
13. Jha, P.A., and A.K. Jha, *Influence of processing conditions on the grain growth and electrical properties of barium zirconate titanate ferroelectric ceramics*. Journal of Alloys and Compounds, 2012. **513**: p. 580–585.
14. Binhayeeniyi, N., P. Sukvisut, C. Thanachayanont, and S. Muensit, *Physical and electromechanical properties of barium zirconium titanate synthesized at low-sintering temperature.* Materials Letters, 2010. **64**(3): p. 305–308.
15. Liu, L., S. Zheng, Y. Huang, D. Shi, S. Wu, L. Fang, C. Hu, B. Elouadi, *Structure and piezoelectric properties of $(1-0.5x)BaTiO_3$–$0.5x$ $(0.4BaZrO_3$–$0.6CaTiO_3)$ ceramics*. Journal of Physics D: Applied Physics, 2012. **45**(29): p. 295403.
16. Jain, A., A.K. Panwar, and A.K. Jha, *Effect of ZnO doping on structural, dielectric, ferroelectric and piezoelectric properties of $BaZr_{0.1}Ti_{0.9}O_3$ ceramics*. Ceramics International, 2017. **43**(2): p 1948–1955.
17. Kumar, D., R. Sagar Yadav, Monika, A. Kumar Singh, and S. Bahadur Rai, *Synthesis Techniques and Applications of Perovskite Material*. Perovskite Materials, Devices and Integration. 2020, IntechOpen.
18. Islam, S., M. R. Molla, N. Khatun, N. I. Tanvir, M. Hakim and Md. S. Islam, *Exploring the effects of zirconium doping on barium titanate ceramics: structural, electrical, and optical properties.* Material Advances, 2025. **6**: p. 1403-1413.
19. Hao, T., J. Shen, Q. Peng, J. Liu, W. Hu, C. Zhong, *Solid-State Synthesis for High-Tetragonality, Small-Particle Barium Titanate.* Materials, 2024. **17**: p. 5655.
20. Dzunuzovic, A.S., M.M.V. Petrovic, J.D. Bobic, N. I. Ilic and B. D. Stojanovicet, *Influence of ferrite phase on electrical properties of the barium zirconium titanate based multiferroic composites*. Journal of Electroceramics,2021. **46:** p. 57–71.
21. Reddy, S.B., K.P. Rao, and M.S.R. Rao, *Nanocrystalline barium zirconate titanate synthesized at low temperature by an aqueous co-precipitation technique.* Scripta Materialia, 2007. **57**(7): p. 591–594.
22. Deluca, M., C.A. Vasilescu, A.C. Ianculescu, D. C. Berger, C. E. Ciomaga, L. P. Curecheriu, L. Stoleriu, A. Gajovic, L. Mitoseriu, C. Galassi, *Investigation of the composition-dependent properties of BaTi 1-xZr xO 3 ceramics prepared by the modified Pechini method.* Journal of the European Ceramic Society, 2012. **32**(13): p. 3551–3566.
23. Veith, M., S. Mathur, N. Lecerf, V. Huch and T. Decker, Sol-gel synthesis of nano-scaled $BaTiO_3$, $BaZrO_3$ and $BaTi_{0.5}Zr_{0.5}O_3$ oxides via single-source alkoxide precursors and semi-alkoxide routes. Journal of Sol-Gel Science and Technology, 2000. **17**(2): p. 145–158.
24. Yoshimura, M., M. Kakihana, and K. Sardar, *A review on the designing of homogeneous multicomponent oxides via polymer complex method*. Materials and Design, 2024. **244**: p. 113118.
25. Nicollet, C., and A.J. Carrillo, *Back to basics: synthesis of metal oxides*. Journal of Electroceramics, 2023. **52**: p.10-28 .
26. Aktaş, P., *Synthesis and Characterization of Barium Titanate Nanopowders by Pechini Process.* Celal Bayar University Journal of Science, 2020. **16**(3): p. 293-300.

27. Upadhyay, R.H., A.P. Argekar, and R.R. Deshmukh, *Characterization, dielectric and electrical behaviour of $BaTiO_3$ nanoparticles prepared via titanium(IV) triethanolaminato isopropoxide and hydrated barium hydroxide*. Bulletin of Material Sciences, 2014. **37**(3): p.481-489
28. Upadhyay, R.H., and R.R. Deshmukh, *A new low dielectric constant barium titanate - poly (methyl methacrylate) nanocomposite films.* Advances in Materials Research, 2013. **2**(2): p. 99–109.
29. Kong, L., I. Karatchevtseva, M. Blackford, I. Chironi, and G. Triani, *Synthesis and characterization of rutile nanocrystals prepared in aqueous media at low temperature*. Journal of the American Ceramic Society, 2012. **95**(2): p. 816–822.
30. Kong, L., I. Karatchevtseva, R. Holmes, J. Davis, Y. Zhang, and G. Triani, *New synthesis route for lead zirconate titanate powder*. Ceramics International, 2016. **42**(6): p. 6782–6790.
31. Match! - Phase Identification from Powder Diffraction, Crystal Impact - Dr. H. Putz & Dr. K. Brandenburg GbR, Kreuzherrenstr. 102, 53227 Bonn, Germany, http://www.crystalimpact.com/match.
32. F. Menges, Spectragryph-optical spectroscopy software, Version 1.2.16.1., 2022.
33. Bernardi, M.I.B., E. Antonelli, A.B. Lourenço, C.A.C. Feitosa, L.J.Q. Maia, and A.C. Hernandes, *$BaTi_{1-x}Zr_xO_3$ nanopowders prepared by the modified Pechini method.* Journal of Thermal Analysis and Calorimetry, 2007. **87**(3): p. 725–730.
34. Chen, X., X. Chao, and Z. Yang, *Submicron barium calcium zirconium titanate ceramic for energy storage synthesised via the co-precipitation method.* Materials Research Bulletin, 2019. **111**: p. 259–266.
35. Reda, M., S.I. El-Dek, and M.M. Arman, *Improvement of ferroelectric properties via Zr doping in barium titanate nanoparticles*. Journal of Materials Sciences: Materials in Electronics, 2022. **33**: p. 16753–16776.